RiCE: Research in Chemical Engineering

Volume 5. No 1, 2026

Journal homepage: https://ejournal.ump.ac.id/index.php/rice

Application of Sol-Gel Synthesized Cu-TiO_2/ZnO Photocatalyst for Textile Dye Wastewater Treatment

David Kevin[1*]

[1]Chemical Engineering Department, Faculty of Engineering, Singaperbangsa University of Karawang
Jl. HS. Ronggowaluyo Telukjambe Timur Karawang 41361

*Corresponding author: *dk0365671@gmail.com*

Article Info

Submited:
02 December 2025

Revised:
08 January 2026

Accepted:
20 January 2026

ABSTRACT

The textile dyeing industry is the second largest water polluter in the world, with the industry generating 20% of the world's total wastewater effluent. Methylene blue is one of the most commonly used textile dyes, causing degradation of aquatic ecosystem quality. A new method that can help in the treatment process of liquid waste that has a relatively low cost, one of which is a photocatalyst using material Cu-TiO_2/ZnO and using the sol gel method. This photocatalyst was tested by characterization using SEM, UV-Vis DRS, and UV-Vis Spectrometer. The results of SEM characteristics show that the particles are spherical with varying particle sizes. The UV-Vis DRS results show that the Eg values obtained are 3.186 eV forTiO_2/ZnO , 2.296 eV for Cu(5%)- TiO_2/ZnO , and 2.162 eV for Cu(8%)- TiO_2/ZnO . The concentration of methylene blue affects the effectiveness of degradation with the highest degradation at 5 ppm of 77.51%, at 10 ppm of 67.02% and 15 ppm of 54.30%. In conclusion, the sol-gel synthesized Cu-TiO_2/ZnO photocatalyst demonstrates promising effectiveness for textile dye wastewater treatment, with optimized Cu doping significantly enhancing visible-light absorption and degradation efficiency of methylene blue.

Keywords: Industry, Methylene Blue, Photocatalyst

1. INTRODUCTION

Industry in Karawang Regency has experienced rapid growth in recent years, so that industrial estates can be formed in a short time. Companies are classified according to the type of industrial products, including metal machinery, various electronic products, mechanical engineering, chemicals, transportation equipment, textiles, paper, agricultural fur products, and forest products [1]. One industry that can cause water pollution is the textile industry. The textile dyeing industry is the second largest water polluter in the world, with the industry generating 20% of the world's total liquid waste [2]. The rapid growth of the textile industry in Indonesia has caused adverse impacts on the environment, mainly due to the discharge of organic liquid waste from factories containing hazardous and toxic substances [3]. The problem is currently faced by countries that depend on the textile dyeing industry, such as China, Thailand and Indonesia. The textile industry is one of the main contributors, producing about 80% of the global synthetic azo dyes [4], of which 10 to 15% of the total dyes used are not bound to the fiber and are directly discharged into the environment [5]. Methylene blue is one of the most commonly used textile dyes, causing

degradation of aquatic ecosystem quality by reducing light penetration and oxygen solubility, and having a negative impact on photosynthesis of aquatic organisms. Commonly used dyes can disrupt aquatic ecosystem processes by reducing oxygen solubility and light penetration, thus affecting photosynthesis and water quality. Water pollution by these dyes can have a very harmful impact on humans, the environment, and aquatic life [5].

The condition of water pollution due to textile waste is a serious problem in Indonesia, especially in industrial areas such as Karawang. Karawang is one of the largest industrial areas in West Java which is the largest manufacturing activity center in Southeast Asia, including the textile industry. The high level of production activity causes an increase in the volume of waste discharged into the environment. Research shows the presence of microplastic contamination in refill drinking water in Karawang as evidenced by the discovery of microplastics in human feces and place. Another industrial wastewater treatment research in Karawang recorded a decrease in nickel levels from 0.016 to 0.006mg/L after treatment, but other metal levels still have the potential to pollute if treatment is not optimal [1].

The treatment of wastewater containing synthetic dyes has been widely carried out, for example through physical methods such as adsorption or biologically using Pseudomonas sp. Various studies report a decrease in the concentration of synthetic dyes in the waste after the process. However, there are still some obstacles both during and after the treatment process. Therefore, it is necessary to develop new methods that are easy to apply and have relatively low costs, one of which is photodegradation using photocatalysts [3].

Photocatalysis, a green chemistry technology, has attracted a lot of attention because of the new materials that have the potential for wastewater treatment [4], [6], including textile dye effluents. The photocatalytic concept involves a semiconductor absorbing photon energy and generating electron-hole pairs, where excited electrons jump from the valence band to the conduction band to cross the band gap. Photocatalysis involves a redox reaction, where electrons act as reducing agents while positive holes act as oxidation sites. Water and oxygen molecules or oxygen-carrying reagents are adsorbed on the catalyst surface to generate hydroxyl radicals (HO-) and reactive oxygen radicals (ROS) [7]. The dye pollutants adsorbed on the catalyst surface are decomposed by HO- and ROS into less harmful compounds or mineralized into harmless $CO_2$and water. Photocatalyst materials such as TiO_2 and ZnO have been investigated for their chemical stability, low toxicity, and photocatalytic efficiency [8], [9]. Their combination in the form of type II heterojunction (TiO_2/ZnO) has been shown to decrease the rate of electron-hole pair recombination and increase reaction efficiency [10], [11]. Structural modification through doping transition metals such as copper (Cu) has shown potential in lowering the band gap energy and extending the light absorption capability into the visible region [12], [13].

Although TiO_2/ZnO heterojunctions and metal doping have been explored separately, research specifically incorporating Cu metal doping into TiO_2/ZnO systems in dye degradation application research using the sol-gel method is still very limited. Not many studies have systematically evaluated the effect of Cu doping on changes in electronic structure, photoreactivity, and degradation efficiency in Cu-TiO_2/ZnO-based PFC systems. In this study, modification of the TiO_2/ZnO heterojunction structure by Cu metal doping can reduce the band gap energy and expand the absorption of light spectrum to the visible region. Thus, the photocatalytic activity of Cu-TiO_2/ZnO system

towards Methylene blue degradation will increase significantly compared to the system without dopant.

Therefore, this study aims to synthesize and evaluate the photocatalytic performance of Cu-doped TiO_2/ZnO heterojunction catalysts prepared via the sol-gel method for the degradation of methylene blue in a Photocatalytic Fuel Cell (PFC) system. Specifically, the research objectives are to: (1) characterize the structural, morphological, and optical properties of the synthesized Cu-TiO_2/ZnO composites; and (2) investigate the effect of methylene blue concentration and operational parameters on the degradation efficiency and electrical output of the PFC.

2. MATERIALS AND METHODS

2.1 Materials

The materials used were methylene blue ($C_{16}H_{18}N_3SCl$, Merck, Germany), ZnO (zinc oxide, p.a, Merck, Germany), TiO_2 (titanium dioxide, p.a, Merck, Germany), KCl (potassium chloride, p.a, Merck, Germany), NaClO (sodium hypochlorite, p.a, 12%), Agar, Distilled water, Graphite plates, Wires, Copper(II) acetate monohydrate ($Cu(CH_3COO)_2$-H_2O) from Supelco, USA, Isopropyl alcohol 99%, Polyethylene glycol (PEG) 400, Glass plates measuring 5 × 3 cm with a thickness of 3 mm.

2.2 Experimental procedure

2.2.1. Synthesis of ZnO

ZnO synthesis was carried out using the sol-gel method. Dissolve 2.743 grams of ZnO into 50 mL of isopropyl alcohol in a 100 mL beaker. Cover the solution with aluminum foil, then stir using a magnetic stirrer for ± 45 minutes. Mix monoethanolamine as much as 1.4 mL and continue stirring for ± 45 minutes. Let the solution stand overnight until sol is formed. Mix PEG as much as 4.4 mL, then stir until homogeneous. Heat the oven to 150°C and put the ZnO sol solution for 2 hours into the oven. After completion, let the solution cool down. Apply the homogeneous ZnO paste to the glass plate using the doctor blade method. Dry the plate in the oven at 200°C for 25 minutes.

2.2.2. Synthesis of Cu-TiO_2/ZnO

Synthesis of Cu-doped TiO_2, using the sol-gel method. Dissolve 2.743 grams of TiO_2 in 50 mL of isopropyl alcohol. Cover the solution with aluminum foil and stir for ± 45 minutes. Add copper (II) acetate monohydrate as dopant in concentrations of 2% [14], 5% [15], and 10% to the mass of TiO_2, then stir for ±45 minutes. Add monoethanolamine as much as 1.4 mL, then stir again for ± 45 minutes until a sol solution is formed. Let the solution stand overnight. Add PEG as much as 4.4 mL, stir until homogeneous. Ovenize the solution at 150 °C for 2 hours, then let it cool. Apply the homogenized Cu-TiO_2 paste to the ZnO-coated glass plate using the doctor blade method. Dry the plate in the oven for 2 hours with temperature variations of 175°C, 200°C, and 225°C.

2.2.3. Preparation of Cathode Plate

Graphite plates measuring 5×4 cm and 3 mm in thickness were used as cathodes. These plates were soaked in NaClO solution before use.

2.2.4. Preparation of Sodium Hypochlorite Solution

A total of 200 mL of NaClO solution was mixed with distilled water to reach a volume of 800 mL. The final concentration of the solution was 250 mL/L.

2.2.5. Preparation for Salt Bridge

The salt bridge was made from 1 M KCl solution by dissolving 1.86 grams of KCl in 25 mL of water, then adding 0.93 grams of agar. The solution was stirred while heated to boiling. After cooling slightly, the solution was put into a pipe and stored in a refrigerator until it thickened.

2.2.6. Methylene blue solution preparation

A stock solution of 100 mL (1,000 ppm) was prepared by dissolving 0.10 grams of methylene blue in 100 mL of distilled water. For

the degradation experiments, methylene blue solutions with three different concentrations (5, 10, and 15 ppm) were prepared by appropriate dilution of the stock solution. To make a 10 ppm solution, take 10 mL of stock solution, add variations of 15, 20 and 25 mL of 10% HCl, then add distilled water until the volume reaches 1,000 mL. The same method is done for a concentration of 5 ppm by taking 5 mL of stock solution and a concentration of 15 ppm by taking 15 mL of stock solution.

2.2.7. Preparation of Double Space PFC

The photoreactor consists of two chambers (anode and cathode) filled with 400 mL of methylene blue solution and 400 mL of NaClO solution, respectively. The two chambers are connected by a KCl-based salt bridge. $CuTiO_2$/ZnO plates were placed in the anode chamber and graphite plates in the cathode chamber, then connected to a multimeter. The anode plate was irradiated using a 100 W UV lamp for 2 hours. Samples of the solution were taken every 40 minutes, filtered once using filter paper, then measured the pH using a pH meter. A total of 5 mL of solution was measured for absorbance using a UV-Vis spectrophotometer at a wavelength of 300-700 nm. The degradation efficiency was calculated using Equation (1):

$$Degradation\ (\%) = \frac{C_0 - C_t}{C_0} x\ 100\% \qquad (1)$$

Where C_0 and C_t are the initial concentration, and concentration after irradiation time (t) respectively.

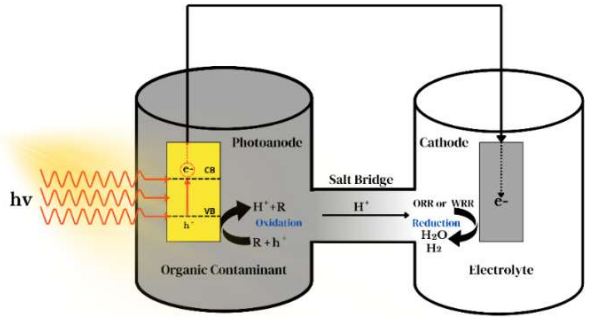

Figure 1. Dual Chamber Photocatalytic Fuel Cell (PFC) System

2.2.8. Photocatalyst Characterization

Characterization of the surface morphology of Cu-TiO_2/ZnO photocatalysts was performed using Scanning Electron Microscopy (SEM) to determine the shape, particle size, and agglomeration level of the synthesized samples with Cu mass variation. Model SU3500 (Hitachi, Japan), with 6.0 mm resolution at 7.00 kV and 10.0k magnification. The optical properties of the synthesized Cu-TiO_2/ZnO photocatalyst material were characterized using UV-Vis Diffuse Reflectance Spectroscopy (DRS) method. This characterization aims to evaluate the light absorption ability and determine the band gap energy value of the material. Model Cary 60 (China), with a wavelength range of 200-830 nm. Measurement of methylene blue absorbance to calculate the degradation efficiency using a UV-Visible spectrophotometer model V-730 (Jasco, Japan), with a wavelength range of 300-700 nm.

3. RESULTS AND DISCUSSION

3.1. Analysis by SEM

Figure 2 and Figure 3 show SEM images of Cu(2%)-TiO_2/ZnO, Cu(5%)-TiO_2/ZnO, and Cu(8%)-TiO_2/ZnO composites coated on glass plates, respectively. In Figure 2, the surface morphology of Cu(2%)-TiO_2/ZnO shows spherical particles with varying particle sizes and irregular structures. Particle agglomeration in this sample is relatively low, and indicates that the particles are still fairly evenly dispersed.

Based on Figure 3 shows the morphology of Cu(5%)-TiO_2/ZnO with a particle shape that tends to be round but irregular. Compared to Cu(2%)-TiO_2/ZnO, this sample shows a higher degree of agglomeration, which indicates the start of the formation of large particles due to the process of unification between particles.

Based on Figure 4 for the Cu(8%)-TiO_2/ZnO composite shows morphology with particle shapes that also tend to be round but irregular. Although the particle size appears smaller, particle agglomeration occurs more significantly. This indicates that increasing Cu concentration has an effect on the formation of larger agglomerates, due to increased interactions between particles.

The level of agglomeration that increases as the mass of Cu increases can be explained by the tendency of TiO_2nanoparticles to be in an unstable condition in dispersed form, so that particles tend to gather in achieving a stable condition [16]. Agglomeration is the process of clumping of small or fine particles into large particles [17]. The main causes of agglomeration include large surface area, surface tension, attractive forces between nanoparticles and oxidation processes [18]. This agglomeration has the potential to decrease the active surface area and reduce the availability of active sites for the photocatalytic process, as well as inhibit the absorption of light and methylene blue molecules during the degradation process [19], [20]. Doping Cu^{2+} ions into the TiO_2structure causes changes in morphology and crystal structure. Partial substitution of Ti^{4+} ions by Cu^{2+}causes deformation of the crystal lattice due to differences in charge and ion size, which results in charge compensation in the form of oxygen vacancy formation [21]. These vacancies have a role in the enhancement of photocatalytic activity through band gap shifts and changes in the electronic structure of the material [22], [23].

Interestingly, the typical ZnO structure in the form of hexagonal shape (wurtzite), which is generally stable at room temperature, was not explicitly observed in the SEM images of the three Cu mass variations. The invisibility of the hexagonal shape of ZnO may be due to several factors, such as the Cu-TiO_2layer being too thick, covering the ZnO surface and changing the overall morphology of the material [24]. In addition, the interaction between Cu ions and the ZnO surface can affect its crystal structure, disrupting the regularity of the wurtzite shape that should be visible [25]. The wurtzite structure of ZnO has the function of providing morphological stability through uniform particle distribution as well as increased specific surface area. Therefore, the loss of ZnO's distinctive structural features can have implications for photocatalytic performance, especially if the cover layer inhibits charge transfer or reduces the exposure of the ZnO active surface [26].

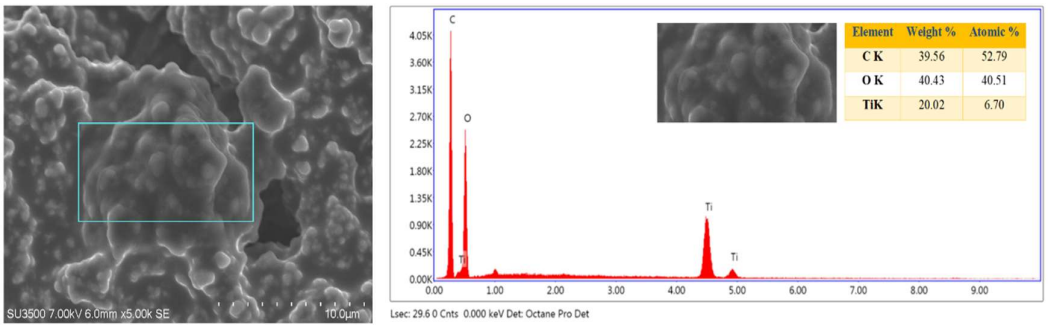

Figure 2. SEM of Cu(2%)-TiO_2/ZnO [24]

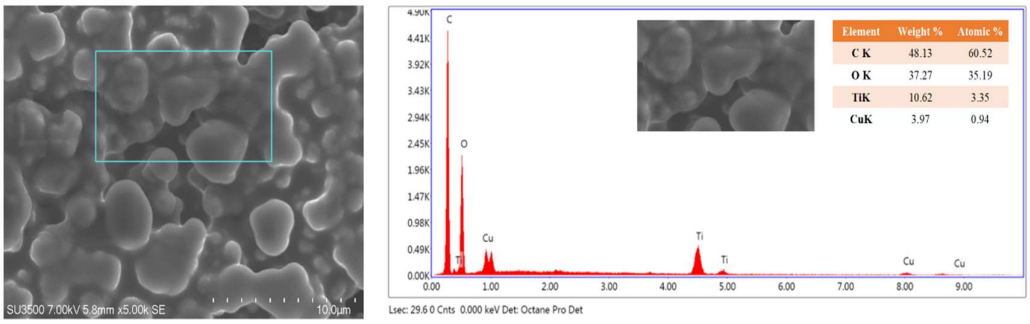

Figure 3. SEM of Cu(5%)-TiO_2/ZnO [24]

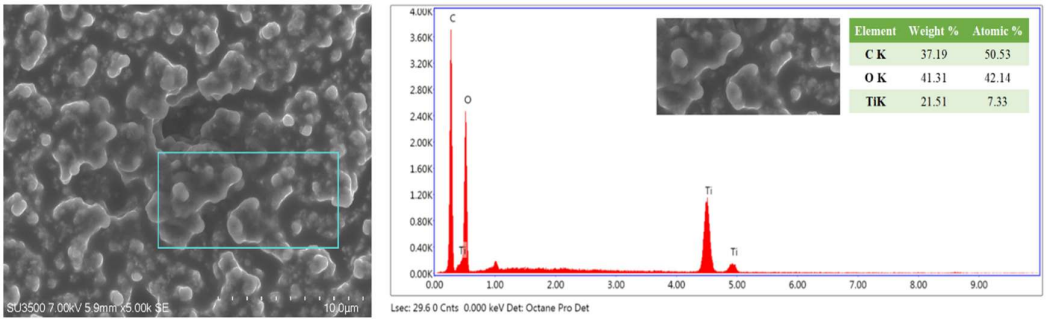

Figure 4. SEM of Cu(8%)-TiO_2/ZnO [24]

3.2. UV-Vis DRS Analysis

UV-visible diffuse reflectance spectra (UV-Vis DRS) is an excellent method to evaluate the light absorption ability of a material. As shown in Figure 5 (b), the UV Vis DRS of Cu(5%)-TiO_2/ZnO, up to Cu(8%)-TiO_2/ZnO shows that there is a significant increase in absorption in the visible light region compared to pure TiO_2/ZnO. This increase in uptake indicates better photocatalytic performance under visible light for Cu(5%)-TiO_2/ZnO, and Cu(8%)-TiO_2/ZnO heterojunctions.

In addition, the bandgap (Eg) values of the synthesized Cu-TiO_2/ZnO photocatalysts were estimated using the Kubelka-Munk approach. The Eg values obtained were 3.186 eV for TiO_2/ZnO, 2.296 eV for Cu(5%)-TiO_2/ZnO, and 2.162 eV for Cu(8%)-TiO_2/ZnO. These results indicated that Cu doping significantly decreased the band gap values of the developed photocatalyst systems [24].

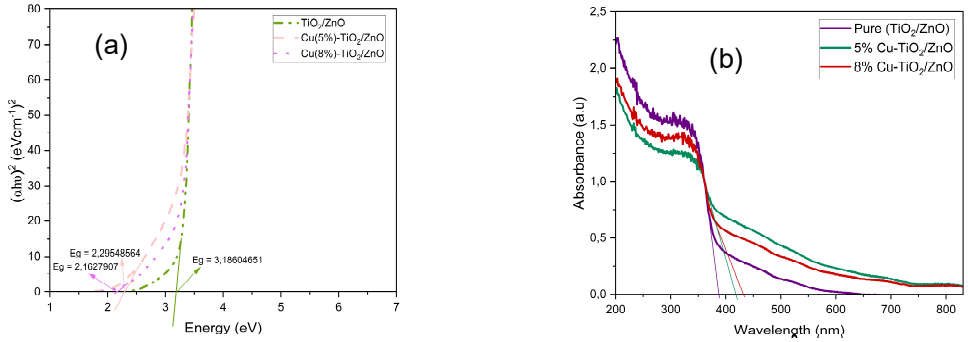

Figure 5. (a) Band gaps for $TiO_{(2)}$/ZnO, Cu(5%)-TiO_2/ZnO, Cu(8%)-$TiO_{(2)}$/ZnO (b) UV-vis spectrum of DRS.

Effect of adding mass variation of Cu doped into TiO_2/ZnO. Figure 5 shows that the decrease in band gap value indicates the successful incorporation of Cu ions into the TiO_2/ZnO semiconductor lattice. Cu acts as a dopant that introduces energy levels between

the valence band and the conduction band, and produces oxygen vacancies, thereby increasing visible light absorption. Cu^{2+}acts as an electron mediator capable of capturing excited electrons, extending the life of holes, and reducing the rate of electron-hole pair recombination[27] . $Ti^{4+}$and Cu^{2+}have similar ionic radii, so Cu^{2+}can easily penetrate the $TiO^{(2)}$matrix as an inner acceptor that interacts with surrounding oxygen vacancies or replaces the position of Ti^{4+} [28]. In addition, modification with Cu shifts the adsorption edge of the photocatalyst towards the visible light region [29] . Studies show diverse speciation on Cu-TiO_2, with most studies reporting the presence of Cu in the Cu^{2+}valence. This species displaces $Ti^{4+}$and increases the density of the oxygen vacancy lattice [30] . In addition, the charge transfer mechanism in the TiO_2/ZnO heterojunction structure enhanced by Cu doping exhibits a Z-scheme, where electrons from the TiO_2 conduction band are transferred to holes in the ZnO valence band, enabling better charge separation [31].

3.3. UV-Vis Spectrometer Analysis

3.3.1. Photocatalyst Performance Test for Photocatalytic Fuel Cell (PFC)

Photocatalyst performance test was conducted to assess the ability of Cu-TiO_2/ZnO material in producing electric voltage when used in Photocatalytic Fuel Cell (PFC) system. The voltage was measured for 120 minutes every 40 minutes interval using a multimeter. Voltage has a significant influence on the degradation results in the photocatalysis process because it is directly related to the separation efficiency of electron-hole pairs formed during excitation by light. The voltage generated by the Photocatalytic Fuel Cell (PFC) system shows a close correlation with the effectiveness of methylene blue (MB) degradation. The voltage measured on the multimeter is a direct indicator of the electron flow generated during the photocatalytic process. The higher the voltage generated, the more efficient the electron transfer process from the CuTiO_2/ZnO photoanode to the graphite cathode, reducing the possibility of recombination between the two.

The resulting voltage was measured using a multimeter to assess the ability of the photocatalyst to convert light energy into electrical energy through redox reactions. The voltage measurement results for HCl vaporization at each time are shown in Table 1. The voltage measurements at various volumes of HCl show varying results during the degradation process. In the use of 15 mL HCl, the voltage generated at the 0th minute or at the beginning of degradation was 0.340 V, remained at 0.340 V until the 40th minute, then increased to 0.408 V at the 80th minute, and reached 0.424 V at the 120th minute. For 20 mL HCl, the initial voltage at the 0th minute was 0.420 V, then decreased to 0.408 V at the 40th minute, 0.396 V at the 80th minute, and remained 0.396 V until the 120th minute. Meanwhile, when using 25 mL HCl, the voltage generated at the 0th minute was 0.432 V, decreased to 0.332 V at the 40th minute, 0.272 V at the 80th minute, and slightly increased to 0.320 V at the 120th minute.

Table 1. Voltage Data for Each HCl Variation

HCl (mL)	Voltage			
	0 minutes	40 minutes	80 minutes	120 minutes
15	0.34	0.34	0.408	0.424
20	0.42	0.408	0.396	0.396
25	0.432	0.332	0..272	0.32

Photocatalyst activity is strongly influenced by the surface area of the glass used as a coating medium. The glass has an important role as a base or support in

distributing the photocatalyst evenly [32] . In order for the photocatalyst to be activated, the glass plate that has been coated with the photocatalyst requires optimal light penetration. The voltage can be as the concentration of pollutants decreases during the photodegradation process. For example, when the solution becomes clearer due to the degradation of methylene blue, the resulting voltage can increase [32].

3.3.2. Photocatalyst Activity

Photodegradation removal efficiency (%) was carried out using Cu(5%)-TiO_2/ZnO composites irradiated with UV light for 120 min. This photocatalyst activity test was conducted on methylene blue waste with concentration variations of 5, 10 and 15 ppm in the anode chamber with Cu-TiO_2/ZnO semiconductor material for a range of 0, 40, 80, and 120 minutes. Figure 6 shows the relationship of irradiation time to degradation rate. The curve shows that the percentage of degradation increases as the UV irradiation time increases with the resulting time occurring within 60 and 120 minutes applicable to all concentrations of methylene blue used [26].

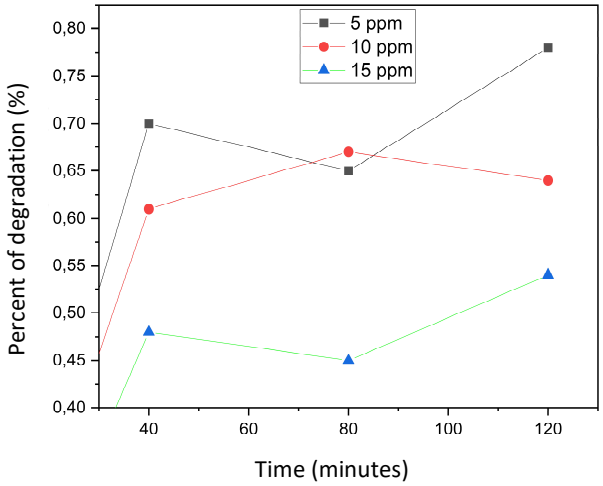

Figure 6. Curve of the Relationship between Duration of Irradiation and %Degradation at Methylene Blue Concentration [33]

The curve in

Figure ***6***, showing the effect of methylene blue concentration on the percentage of degradation by making methylene blue concentrations of 5, 10 and 15 ppm shows that the greater the concentration of methylene blue, the lower the degradation rate, this is similar to the findings of [34] which reports the results of irradiation with a decrease in dye concentration shows results reaching 90%, that increasing the concentration of methylene blue causes the length of the photon path that illuminates the solution thereby reducing the intensity of light needed to reach the catalyst. As a result, only a fraction of the light is effective in the photocatalysis process and the rate of methylene blue degradation. The length of time irradiated by UV light proves that there is an interaction between the Cu-TiO_2/ZnO composite material and methylene blue so that it causes the species h^+_{vb} or -OH radicals formed on the surface of the photocatalyst to increase and the interaction between the photocatalyst and methylene blue is also longer so that it will increase the effectiveness of photodegradation. The phenomenon of the length of irradiation is in line with the findings of previous researchers who reported the

length of irradiation in this study which is 360 minutes produced the best [35]

As the dye concentration was increased, the photodegradation rate decreased. As the initial concentration of dye increases, the path length of photons entering the solution decreases, leading to a reduced number of photons reaching the catalyst surface. Conversely, at lower dye concentrations the opposite effect occurs leading to an increase in the number of photons absorbed by the catalyst at lower concentrations [34].

3.3.3. Kinetic Study

A first order Langmuir-Hinshelwood (LH) kinetic model was followed to determine the change in MB concentration [36]

$$ln\, C_t = -kt + ln\, C_0 \quad (2)$$

$$ln \frac{C_0}{C_t} = kt \quad (3)$$

The experimental data were plotted and linearized on Figure 7, where the slope refers to the concentration-dependent degradation rate constant. A steeper slope indicates a higher rate constant and better photodegradation efficiency. The half-life was also determined based on 0.693/k to determine the time required for the MB concentration to decrease to half of the initial concentration. The experimental results were in good agreement with the linearized model with R^2 ranging from 0.64855 to 0.73422.

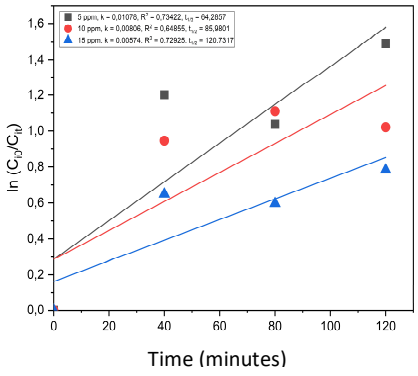

Figure 7. First-order linear regression of MB photodegradation kinetic data under UV light irradiation for 2 h with Cu(5%)-TiO_2/ZnO samples with different MB concentrations of 5 ppm, 10 ppm, and 15 ppm

3.3.4. Effect of Variation of HCl Addition

Another factor affecting the degradation efficiency is that the addition of HCl solution changes the pH of the solution to acidic (pH = 3). The pH value of the aqueous solution affects the photocatalytic reaction by changing the surface charge, size, and energy band structure of the catalyst [37], [38] . The pH of the solution controls the degree of ionization of methylene blue and the surface charge capacity of the adsorbent determined by the zero charge point (pHpzc)[39] , where the adsorbent surface charge is zero and controls the surface electrokinetic characteristics when OH^-/H^+ is the determining ion [40] . At pH<pHpzc, a protonation reaction occurs, making the catalyst surface positively charged. Whereas at pH>pHpzc a deprotonation reaction occurs which makes the catalyst surface negatively charged [26]. At pH<pHpzc, a protonation reaction occurs and the catalyst surface is positively charged. The deprotonation reaction occurs at pH>pHpzc which makes the catalyst surface negatively charged [40] . Methylene blue as a cationic dye undergoes lower adsorption in acidic state, due to excess H $ions^+$ that compete with methylene blue molecules. This reduces the photocatalytic activity due to saturation and poisoning of the catalyst surface by MB, as well as inhibiting light penetration, a

critical factor in the formation of electron-hole pairs [38]

3.3.5. Photocatalytic Mechanism

The photocatalytic mechanism in the Cu-TiO_2/ZnO system for the degradation of organic compounds such as Methylene blue (MB) takes place through a series of electron excitation processes, charge transfer, and redox reactions on the surface of the photocatalyst. When the Cu-TiO_2/ZnO photocatalyst is exposed to UV light with photon energy (hv) equal to or greater than its bandgap, electron excitation from the valence band (VB) to the conduction band (CB) occurs, leaving holes in the VB[41], [42], [43], [44], [45], [46]

$$Cu - TiO_2/ZnO + hv \rightarrow Cu - TiO_2/ZnO\ (e_{CB}^-, h_{VB}^+) \quad (4)$$

These formed charge pairs (e^- and h^+) further act as reduction and oxidation agents. The hole (h^+) on VB has a high potential to oxidize water molecules or hydroxide ions into hydroxyl radicals (-OH), a highly reactive oxidizing species.

$$h_{VB}^+ + (H_2O) \rightarrow H^+ + \cdot OH \quad (5)$$

These -OH radicals play a major role in degrading MB molecules into simpler compounds such as $CO_2$and H_2O [47], [48] , through multistage oxidation reactions:

$$\cdot OH + C_{15}H_{15}N_3O_2 \rightarrow CO_2 + H_2O + others\ product \quad (6)$$

On the other hand, the excited electrons (e^-) on the CB can move to the surface or to the electrode (if an electrochemical system is used) and reduce the dissolved oxygen (O_2). Under neutral or acidic conditions, oxygen undergoes an oxygen reduction reaction (ORR) [41], [49], [50], [51], [52] , forming H_2O or H_2O_2which also contributes in generating additional hydroxyl radicals:

$$O_2 + 4e^- + 4H^+ \rightarrow 2H_2O \quad (7)$$

$$O_2 + 2e^- + 2H^+ \rightarrow H_2O_2 \quad (8)$$

While in alkaline media, the dominant reaction is water reduction (WRR).

$$H_2O + \frac{1}{2}O_2 + 2e^- \rightarrow 2OH^- \quad (9)$$

If $O_2$is not available, then H^+ ions can be reduced to hydrogen gas.

$$2H^+ + 2e^- \rightarrow H_2 \quad (10)$$

In alkaline media, WRR produces hydrogen through

$$2H_2O + 2e^- \rightarrow H_2 + 2OH^- \quad (11)$$

4. CONCLUSION

This study shows the success of Cu-TiO_2/ZnO semiconductor composite synthesized by sol-gel method which has effective photocatalytic activity in methylene blue degradation. SEM characterization shows that the Cu-TiO_2/ZnO particles are spherical with varying sizes. UV-Vis DRS analysis showed a decrease in energy band gap along with an increase in Cu content, as well as a shift in absorbance wavelength. The Eg values obtained were 3.186 eV for TiO_2/ZnO, 2.296 eV for Cu(5%)-TiO_2/ZnO, and 2.162 eV for Cu(8%)-TiO_2/ZnO. Methylene blue concentration affects the effectiveness of degradation, with the highest degradation at 5 ppm of 77.51%, at 10 ppm of 67.02% and 15 ppm of 54.30%. Another factor that also affects the degradation efficiency is the addition of HCl solution, which causes the solution pH to turn acidic with a pH value of 3.

REFERENCES

[1] A. Z. Wathoni, N. Q. Faagna, and A. I. Pratiwi, "Pengaruh Aktivitas Industri Terhadap Kualitas Air Sungai Kabupaten Karawang," *Ind. Xplore*, vol. 9, no. 1, pp. 368–377, 2024, doi: 10.36805/teknikindustri.v9i1.6486.

[2] J. Stokes, "Textile industry: water management." [Online]. Available: https://pciaw.org/textile-industry-water-management/

[3] S. N. Sakinah, Julinawati, Fathurrahmi, and Sheilatina, "Immobilisasi A-Fe2O3/Bentonit Sebagai Fotokatalis Pada Fotodegradasi Zat Warna Methylene Blue," *J. Glob. Ilm.*, vol. 2, no. 3, pp. 1–10, 2024.

[4] D. Ariyanti, F. Wicaksana, and W. Gao, "Submerged Membrane Photo Reactor (SMPR) with Simultaneous Photo Degradation and TiO2 Catalyst Recovery for Efficient Dyes

Removal," *ASEAN J. Chem. Eng.*, vol. 21, no. 2, 2021, doi: 10.22146/ajche.65952.

[5] M. Ikram *et al.*, "Biodegradation of Azo Dye Methyl Red by Pseudomonas aeruginosa: Optimization of Process Conditions," *Int. J. Environ. Res. Public Health*, vol. 19, no. 16, 2022, doi: 10.3390/ijerph19169962.

[6] S. K. Kamarudin, W. R. W. Daud, M. S. Ayub, A. W. Mohammad, and S. E. Lyuke, "A Review on Fuel Cell as Advanced Power Source," *ASEAN J. Chem. Eng.*, vol. 2, no. 1, 2008, doi: 10.22146/ajche.50806.

[7] M. Fahmi, M. Febriansyah, R. Yudianti, and M. Ibadurrohman, "Comparative study of g- C_3N_4 / Cu_2O and $BiVO_4$ / Cu_2O photocathodes for enhanced electricity generation and hydrogen evolution in photocatalytic fuel cells," vol. 15, no. 1, pp. 191–203, 2026.

[8] S. Babel, P. A. Sekartaji, and H. Sudrajat, "TiO2 as an effective nanocatalyst for photocatalytic degradation of humic acid in water environment," *J. Water Supply Res. Technol. - AQUA*, vol. 66, no. 1, 2017, doi: 10.2166/aqua.2016.102.

[9] A. N. El-Shazly, A. H. Hegazy, E. T. El Shenawy, M. A. Hamza, and N. K. Allam, "Novel facet-engineered multi-doped TiO2 mesocrystals with unprecedented visible light photocatalytic hydrogen production," *Sol. Energy Mater. Sol. Cells*, vol. 220, 2021, doi: 10.1016/j.solmat.2020.110825.

[10] M. M. Ali, M. J. Haque, M. H. Kabir, M. A. Kaiyum, and M. S. Rahman, "Nano synthesis of ZnO–TiO2 composites by sol-gel method and evaluation of their antibacterial, optical and photocatalytic activities," *Results Mater.*, vol. 11, p. 100199, 2021, doi: 10.1016/j.rinma.2021.100199.

[11] N. Suganthi, S. Thangavel, and K. Kannan, "Hibiscus subdariffa leaf extract mediated 2-D fern-like ZnO/TiO2 hierarchical nanoleaf for photocatalytic degradation," *FlatChem*, vol. 24, no. July, p. 100197, 2020, doi: 10.1016/j.flatc.2020.100197.

[12] N. R. Khalid, E. Ahmed, Z. Hong, M. Ahmad, Y. Zhang, and S. Khalid, "Cu-doped TiO2 nanoparticles/graphene composites for efficient visible-light photocatalysis," *Ceram. Int.*, vol. 39, no. 6, 2013, doi: 10.1016/j.ceramint.2013.02.051.

[13] L. Tian, Z. Li, X. Xu, and C. Zhang, "Advances in noble metal (Ru, Rh, and Ir) doping for boosting water splitting electrocatalysis," *Journal of Materials Chemistry A*, vol. 9, no. 23. 2021. doi: 10.1039/d1ta01108a.

[14] S. Preda *et al.*, "Photocatalytic and Antibacterial Properties of Doped TiO2 Nanopowders Synthesized by Sol–Gel Method," *Gels*, vol. 8, no. 10, pp. 1–20, 2022, doi: 10.3390/gels8100673.

[15] A. Adamu, M. Isaacs, K. Boodhoo, and F. R. Abegão, "Investigation of Cu/TiO2 synthesis methods and conditions for CO2 photocatalytic reduction via conversion of bicarbonate/carbonate to formate," *J. CO2 Util.*, vol. 70, 2023, doi: 10.1016/j.jcou.2023.102428.

[16] Nasikhudin, M. Diantoro, A. Kusumaatmaja, and K. Triyana, "Study on Photocatalytic Properties of TiO2 Nanoparticle in various pH condition," in *Journal of Physics: Conference Series*, 2018. doi: 10.1088/1742-6596/1011/1/012069.

[17] T. Degabriel *et al.*, "Factors impacting the aggregation/agglomeration and photocatalytic activity of highly crystalline spheroid- and rod-shaped TiO2 nanoparticles in aqueous solutions," *Phys. Chem. Chem. Phys.*, vol. 20, no. 18, 2018, doi: 10.1039/c7cp08054a.

[18] N. Sondezi, Z. Njengele-Tetyana, K. P. Matabola, and T. A. Makhetha, "Sol-Gel-Derived TiO2 and TiO2/Cu Nanoparticles: Synthesis, Characterization, and Antibacterial Efficacy," *ACS Omega*, vol. 9, no. 14, pp. 15959–15970, 2024, doi: 10.1021/acsomega.3c09308.

[19] F. Pellegrino *et al.*, "Influence of agglomeration and aggregation on the photocatalytic activity of TiO2 nanoparticles," *Appl. Catal. B Environ.*, vol. 216, 2017, doi: 10.1016/j.apcatb.2017.05.046.

[20] D. Sugandi, N. Wahyuni, and W. Rahmalia, "Fotocatalytic degradation of methylene blue by floating TiO2-coconut fiber," *Acta Chim. Asiana*, vol. 7, no. 1, pp. 437–442, 2024, doi: 10.29303/aca.v7i1.183.

[21] M. Sahu and P. Biswas, "Single-step processing of copper-doped titania nanomaterials in a

flame aerosol reactor," *Nanoscale Res. Lett.*, vol. 6, 2011, doi: 10.1186/1556-276X-6-441.

[22] M. R. Delsouz Khaki, M. S. Shafeeyan, A. A. A. Raman, and W. M. A. W. Daud, "Enhanced UV–Visible photocatalytic activity of Cu-doped ZnO/TiO2 nanoparticles," *J. Mater. Sci. Mater. Electron.*, vol. 29, no. 7, 2018, doi: 10.1007/s10854-017-8515-9.

[23] L. Li *et al.*, "Surface doping for photocatalytic purposes: Relations between particle size, surface modifications, and photoactivity of SnO2:Zn 2+ nanocrystals," *Nanotechnology*, vol. 20, no. 15, 2009, doi: 10.1088/0957-4484/20/15/155706.

[24] D. Kevin, "PENGARUH VARIASI MASSA Cu DAN SUHU KALSINASI PADA SINTESIS FOTOKATALIS Cu-TiO2/ZnO UNTUK DEGRADASI METHYLENE BLUE DALAM PHOTOCATALYTIC FUEL CELL (PFC)," *J. Inov. Tek. Kim.*, vol. 10, no. 2, pp. 100–112, 2025, doi: 10.31942/inteka.v10i2.13076.

[25] T. M. Abdel-Fattah, A. Wixtrom, K. Zhang, W. Cao, and H. Baumgart, "Highly Uniform Self-Assembled Gold Nanoparticles over High Surface Area ZnO Nanorods as Catalysts," *ECS J. Solid State Sci. Technol.*, vol. 3, no. 10, 2014, doi: 10.1149/2.0211410jss.

[26] T. S. Putri, S. Dampang, M. F. Hakim, F. Yuliasari, D. Kevin, and C. P. Meylani, "Pengaruh Luas Permukaan Material Fotokatalis Cu-TiO 2 / ZnO dan Larutan HCl Terhadap Degradasi Methylene Blue dalam Photocatalytic Fuel Cell," vol. X, no. 4, pp. 15202–15209, 2025.

[27] X. J. Yang, S. Wang, H. M. Sun, X. B. Wang, and J. S. Lian, "Preparation and photocatalytic performance of Cu-doped TiO2 nanoparticles," *Trans. Nonferrous Met. Soc. China (English Ed.*, vol. 25, no. 2, pp. 504–509, 2015, doi: 10.1016/S1003-6326(15)63631-7.

[28] R. Yusoff *et al.*, "Physical properties of aqueous mixtures of N-methyldiethanolamine (MDEA) and ionic liquids," *J. Ind. Eng. Chem.*, vol. 20, no. 5, pp. 3349–3355, 2014, doi: 10.1016/j.jiec.2013.12.019.

[29] R. Mohan, K. Krishnamoorthy, and S. J. Kim, "Enhanced photocatalytic activity of Cu-doped ZnO nanorods," *Solid State Commun.*, vol. 152, no. 5, pp. 375–380, 2012, doi: 10.1016/j.ssc.2011.12.008.

[30] D. A. H. Hanaor and C. C. Sorrell, "Review of the anatase to rutile phase transformation," *J. Mater. Sci.*, vol. 46, no. 4, pp. 855–874, 2011, doi: 10.1007/s10853-010-5113-0.

[31] R. Zha, R. Nadimicherla, and X. Guo, "Ultraviolet photocatalytic degradation of methyl orange by nanostructured TiO2/ZnO heterojunctions," *J. Mater. Chem. A*, vol. 3, no. 12, 2015, doi: 10.1039/c5ta00764j.

[32] Q. Ayun, R. Ridho, and E. Malis, "Pengaruh Pelapisan Titanium Dioksida (Tio2) Pada Plat Kaca Terhadap Efektivitas Fotodegradasi Methyl Orange Menggunakan Metode Sodis (Solar Disinfection Water)," *J. Cryst. Publ. Penelit. Kim. dan Ter.*, vol. 2, no. 1, pp. 37–50, 2020, doi: 10.36526/jc.v2i1.924.

[33] C. Putri Meylani, Sarah Dampang, Muhammad Fahmi Hakim, Fitri Yuliasari, David Kevin, and Tarishah Setyowati Putri, "Pengaruh Konsentrasi Methylene Blue dan NaClO pada Proses Degradasi Photocatalytic Fuel Cell Menggunakan Elektroda Cu-TiO2/ZnO," *J. Tek. Kim. USU*, vol. 14, no. 2, 2025, doi: 10.32734/jtk.v14i2.20525.

[34] S. K. Kansal, M. Singh, and D. Sud, "Studies on photodegradation of two commercial dyes in aqueous phase using different photocatalysts," *J. Hazard. Mater.*, vol. 141, no. 3, 2007, doi: 10.1016/j.jhazmat.2006.07.035.

[35] S. Sakthivel, B. Neppolian, M. V. Shankar, B. Arabindoo, M. Palanichamy, and V. Murugesan, "Solar photocatalytic degradation of azo dye: Comparison of photocatalytic efficiency of ZnO and TiO2," *Sol. Energy Mater. Sol. Cells*, vol. 77, no. 1, 2003, doi: 10.1016/S0927-0248(02)00255-6.

[36] A. Lau *et al.*, "Visible-light Degradation of Methylene Blue using Energy-Efficient Carbon-Doped TiO2: Kinetic Study and Mechanism," *Bull. Chem. React. Eng. Catal.*, vol. 20, no. 1, pp. 177–192, 2025, doi: 10.9767/bcrec.20347.

[37] H. Chen, N. Chen, Y. Gao, and C. Feng, "Photocatalytic degradation of methylene blue by magnetically recoverable Fe3O4/Ag6Si2O7 under simulated visible light," *Powder Technol.*, vol. 326, 2018, doi: 10.1016/j.powtec.2017.12.029.

[38] T. Fotiou, T. M. Triantis, T. Kaloudis, and A. Hiskia, "Evaluation of the photocatalytic

activity of TiO2 based catalysts for the degradation and mineralization of cyanobacterial toxins and water off-odor compounds under UV-A, solar and visible light," *Chem. Eng. J.*, vol. 261, 2015, doi: 10.1016/j.cej.2014.03.095.

[39] P. O. Oladoye, T. O. Ajiboye, E. O. Omotola, and O. J. Oyewola, "Methylene blue dye: Toxicity and potential elimination technology from wastewater," *Results in Engineering*, vol. 16. 2022. doi: 10.1016/j.rineng.2022.100678.

[40] M. R. Delsouz Khaki, M. S. Shafeeyan, A. A. A. Raman, and W. M. A. W. Daud, "Evaluating the efficiency of nano-sized Cu doped TiO2/ZnO photocatalyst under visible light irradiation," *J. Mol. Liq.*, vol. 258, 2018, doi: 10.1016/j.molliq.2017.11.030.

[41] S. L. Lee *et al.*, "Role of dissolved oxygen on the degradation mechanism of Reactive Green 19 and electricity generation in photocatalytic fuel cell," *Chemosphere*, vol. 194, 2018, doi: 10.1016/j.chemosphere.2017.11.166.

[42] P. Li *et al.*, "Approaches for Enhancing Wastewater Treatment of Photocatalytic Fuel Cells: A Review," *Materials (Basel).*, vol. 17, no. 9, pp. 1–17, 2024, doi: 10.3390/ma17092139.

[43] R. S. Mukkavilli *et al.*, "Electrocatalytic activity, phase kinetics, spectroscopic advancements, and photocorrosion behaviour in tantalum nitride phases," *Nano Energy*, vol. 129, no. May, 2024, doi: 10.1016/j.nanoen.2024.110046.

[44] S. Sehar, F. Sher, S. Zhang, U. Khalid, J. Sulejmanović, and E. C. Lima, "Thermodynamic and kinetic study of synthesised graphene oxide-CuO nanocomposites: A way forward to fuel additive and photocatalytic potentials," *J. Mol. Liq.*, vol. 313, 2020, doi: 10.1016/j.molliq.2020.113494.

[45] H. Tang, K. Geng, Y. Hu, and N. Li, "Synthesis and properties of phosphonated polysulfones for durable high-temperature proton exchange membranes fuel cell," *J. Memb. Sci.*, vol. 605, 2020, doi: 10.1016/j.memsci.2020.118107.

[46] D. Rajamanickam and M. Shanthi, "Photocatalytic degradation of an organic pollutant by zinc oxide – solar process," *Arab. J. Chem.*, vol. 9, 2016, doi: 10.1016/j.arabjc.2012.05.006.

[47] S. L. Lee *et al.*, "Exploring the relationship between molecular structure of dyes and light sources for photodegradation and electricity generation in photocatalytic fuel cell," *Chemosphere*, vol. 209, 2018, doi: 10.1016/j.chemosphere.2018.06.157.

[48] M. A. Rauf and S. S. Ashraf, "Fundamental principles and application of heterogeneous photocatalytic degradation of dyes in solution," *Chemical Engineering Journal*, vol. 151, no. 1–3. 2009. doi: 10.1016/j.cej.2009.02.026.

[49] A. Houas, H. Lachheb, M. Ksibi, E. Elaloui, C. Guillard, and J. M. Herrmann, "Photocatalytic degradation pathway of methylene blue in water," *Appl. Catal. B Environ.*, vol. 31, no. 2, 2001, doi: 10.1016/S0926-3373(00)00276-9.

[50] M. W. Kee, J. W. Soo, S. M. Lam, J. C. Sin, and A. R. Mohamed, "Evaluation of photocatalytic fuel cell (PFC) for electricity production and simultaneous degradation of methyl green in synthetic and real greywater effluents," *J. Environ. Manage.*, vol. 228, 2018, doi: 10.1016/j.jenvman.2018.09.038.

[51] C. B. Ong, L. Y. Ng, and A. W. Mohammad, "A review of ZnO nanoparticles as solar photocatalysts: Synthesis, mechanisms and applications," *Renewable and Sustainable Energy Reviews*, vol. 81. 2018. doi: 10.1016/j.rser.2017.08.020.

[52] K. Zhao *et al.*, "Efficient wastewater treatment and simultaneously electricity production using a photocatalytic fuel cell based on the radical chain reactions initiated by dual photoelectrodes," *J. Hazard. Mater.*, vol. 337, 2017, doi: 10.1016/j.jhazmat.2017.05.004.